JOURNAL OF GEOPHYSICAL RESEARCH, VOL. 113, A06214, doi:10.1029/2007JA012628, 2008

Penetration of magnetospheric electric fields to the equator during a geomagnetic storm

Takashi Kikuchi,[1,3] Kumiko K. Hashimoto,[2] and Kenro Nozaki[3]

Received 4 July 2007; revised 3 November 2007; accepted 11 February 2008; published 14 June 2008.

[1] Penetration of the magnetospheric electric field to the equatorial ionosphere was examined for the geomagnetic storm on 6 November 2001, by analyzing the difference in magnitude of the geomagnetic storm recorded at the dayside geomagnetic equator, Yap (−0.3° GML) and low latitude, Okinawa (14.47° GML). The penetrated electric field caused the DP2 currents at the equator, i.e., eastward currents during the main phase of the storm, while the overshielding currents, i.e., westward currents dominated during the recovery phase. It is shown that the ring current started to develop simultaneously with the onset of the equatorial DP2 within the temporal resolution of a few minutes. These results imply prompt transmission of the dawn-to-dusk convection electric field to the inner magnetosphere as well as to the equatorial ionosphere. It is found that the equatorial DP2 started to decrease one hour after the onset of the ring current development, indicating shielding effects becoming effective at the equator during the latter half of the storm main phase. The DP2 was then overwhelmed by the overshielding, which resulted in the counter electrojet (CEJ) in the beginning of the storm recovery phase. The IMAGE magnetometer chain data indicate that the westward auroral electrojet (AEJ) in the dawn sector was driven over midlatitude centered at 57° corrected geomagnetic latitude (CGML) during the main phase, while the AEJ shifted rapidly poleward to the auroral latitude centered at 67° CGML in the beginning of the recovery phase. The overshielding must be caused by the abrupt poleward shift of the R1 FACs as inferred from the poleward shift of the AEJ, in addition to the decrease in their magnitude due to the decrease in magnitude of the southward IMF. The geomagnetic storm at the dayside geomagnetic equator was enhanced in amplitude with the ratio of 2.7 as compared with the geomagnetic storm at low latitude. This amplification is a result of both effects of the DP2 currents and the CEJ associated with the main and recovery phases, respectively. It is suggested that the electric field associated with the DP2 currents contributed to the development of the ring current during the main phase, while the overshielding electric field may contribute to cease developing the ring current during the recovery phase.

Citation: Kikuchi, T., K. K. Hashimoto, and K. Nozaki (2008), Penetration of magnetospheric electric fields to the equator during a geomagnetic storm, *J. Geophys. Res.*, *113*, A06214, doi:10.1029/2007JA012628.

1. Introduction

[2] It has been well known that the magnetospheric electric field is transmitted promptly to the equator during the geomagnetic perturbations such as the geomagnetic sudden commencements (SCs), geomagnetic pulsations (PCs), quasiperiodic DP2 magnetic fluctuations and substorms [*Nishida et al.*, 1966; *Nishida*, 1968; *Onwumechilli et al.*, 1973; *Araki*, 1977, 1994; *Trivedi et al.*, 1997; *Motoba et al.*, 2002, 2004; *Kikuchi et al.*, 1996, 2000b, 2003]. With high time resolution magnetometer data, it was shown that the polar electric field was transmitted to the equator instantaneously within the temporal resolution of 10s of seconds [*Araki*, 1977; *Kikuchi et al.*, 1996; *Motoba et al.*, 2002]. The instantaneous transmission of the polar electric field was explained by means of the TM_0 mode waves in the Earth-ionosphere waveguide [*Kikuchi et al.*, 1978; *Kikuchi and Araki*, 1979]. *Kikuchi et al.* [1996] suggested that the Region-1 field-aligned currents (R1 FACs) flowed into the equatorial ionosphere via the polar ionosphere, and were amplified by the Cowling effects [*Hirono*, 1952; *Baker and Martyn*, 1953].

[3] During the substorm growth phase, the convection electric fields and the DP2 currents were transmitted to the equatorial ionosphere [*Kelley et al.*, 1979; *Fejer et al.*, 1979; *Gonzales et al.*, 1979; *Somayajulu et al.*, 1987; *Kikuchi et al.*, 2000a]. On the other hand, the enhanced convection causes the plasma sheet plasma to move earthward, driving

[1]Solar-Terrestrial Environment Laboratory, Nagoya University, Nagoya, Aichi, Japan.
[2]School of Environment Management, Kibi International University, Takahashi, Okayama, Japan.
[3]Applied Electromagnetic Research Center, National Institute of Information and Communications Technology, Koganei, Tokyo, Japan.

0148-0227/08/2007JA012628$09.00

a partial ring current due to the gradient and curvature drifts of the plasma and shielding electric fields are built up equatorward of the auroral latitudes [*Vasyliunas*, 1972; *Jaggi and Wolf*, 1973; *Southwood*, 1977; *Senior and Blanc*, 1984]. The timescale of the shielding has been estimated as 17–20 min from the magnetometer observations [*Somayajulu et al.*, 1987; *Kikuchi et al.*, 2000b] and 20–30 min from the theoretical calculations [*Senior and Blanc*, 1984; *Peymirat et al.*, 2000]. After the shielding electric field grows, the electric fields at mid and low latitudes are often reversed when the convection electric field is decreased abruptly because of the northward turning of the IMF [*Rastogi and Patel*, 1975; *Kelley et al.*, 1979; *Fejer et al.*, 1979; *Gonzales et al.*, 1979; *Kobea et al.*, 2000; *Kikuchi et al.*, 2000b, 2003]. The reversal of the penetrated electric field was identified as the overshielding electric field [*Kelley et al.*, 1979; *Gonzales et al.*, 1979; *Fejer et al.*, 1979] and the reversed currents that appear at the equator as the counter-electrojets (CEJ) [*Rastogi and Patel*, 1975, 1977, 1997; *Kobea et al.*, 1998, 2000; *Kikuchi et al.*, 2000b, 2003].

[4] During the geomagnetic storm, the DP2 currents flowed into the mid to equatorial latitude ionosphere [*Wilson et al.*, 2001; *Tsurutani et al.*, 2004; *Huang et al.*, 2005]. *Wilson et al.* [2001] demonstrated that intensified DP2 currents were observed at midlatitude during a major geomagnetic storm, when a significant electric field was detected by CRRES inside the ring current. Likewise, the stormtime electric field has been observed in the inner magnetosphere by CRRES and Akebono satellites at L values of 2–6 [*Wygant et al.*, 1998; *Burke et al.*, 1998; *Shinbori et al.*, 2005]. *Shinbori et al.* [2005] showed temporal variations of the electric field at a distance of 2.5 Re during the main phase of the geomagnetic storm on 13 March 1989, with magnitude of up to 46 mV/m. *Wilson et al.* [2001] suggested that the ionospheric electric field responsible for the DP2 currents may have contributed to the development of the storm ring current.

[5] The convection electric field was directly observed with the incoherent scatter radars at Milstone Hill and Jicamarca [*Huang et al.*, 2005]. *Huang et al.* [2005] suggested that the shielding was not effective for many hours during the storm main phase. On the other hand, the penetrated electric field reversed its direction during the storm because of the northward turning of the IMF, which caused the equatorial counter-electrojet [*Rastogi*, 1977]. As a result, the amplitude of the geomagnetic storm was significantly enhanced at the dayside equator [*Rastogi*, 2004]. The reversed electric field was observed in the inner magnetosphere by CRRES during the recovery phase of the storm [*Wygant et al.*, 1998]. The reversed electric field associated with the storm was attributed to the disturbance dynamo, the solar wind dynamo driven by the northward IMF and/or the overshielding due to the R2 FACs [*Huang et al.*, 2001, 2005; *Tsurutani et al.*, 2004].

[6] The magnetospheric electric field commonly penetrates to the equatorial ionosphere during a geomagnetic storm as mentioned above, however, there remain several questions on the storm-time electric and magnetic fields at the equator. The first question is on the relationship between the DP2 currents and the development of the ring current, particularly, on the onset times of these disturbances. The second is the growth time of the shielding electric field which was several hours for the storm main phase [*Huang et al.*, 2005], although the shielding time was about 20 min for the substorm [*Somayajulu et al.*, 1987; *Kikuchi et al.*, 2000b]. The third is the cause of the overshielding during the storm, which was attributed to the northward turning of the IMF [*Rastogi*, 2004]. The fourth is the equatorial enhancement of the geomagnetic storm, which was attributed to the counter electrojet during the storm main phase [*Rastogi*, 2004].

[7] To answer these questions, we analyzed the geomagnetic storm characterized by the well defined onset of the ring current and of the equatorial DP2, using magnetometer data from the geomagnetic equator (Yap, −0.3° GML) and low latitude (Okinawa, 14.47° GML). The magnetometer data at Okinawa was used as a reference for calculation of the equatorial DP2, since Okinawa is located outside the equatorial electrojet and far from the high latitude geomagnetic disturbances. We found that the DP2 was considerably enhanced at the geomagnetic equator during whole two hours of the storm main phase, which was followed by reversed currents, CEJ, during the first three hours of the storm recovery phase. We show that the onsets of the equatorial DP2 and of the SYM-H representing the ring current were simultaneous within a few minutes, and that the equatorial DP2 decreased substantially one hour after the SC. With these results, we discuss prompt penetration of the convection and shielding electric fields to the inner magnetosphere as well as to the equator. In particular, the shielding became effective during the latter half of the storm main phase. We further examined the storm phase dependence of the latitude of the auroral electrojet (AEJ) in the dawn sector using the IMAGE chain magnetometer data. The westward AEJ developed at midlatitude (57° CGML) from the beginning of the storm and shifted rapidly poleward by 10° at the beginning of the recovery phase. The overshielding could be closely related to the abrupt poleward shift of the R1FACs as inferred from the location of the AEJ. We finally show that both the DP2 during the main phase and the CEJ during the recovery phase contributed to amplify the geomagnetic storm at the dayside geomagnetic equator.

2. Geomagnetic Storm on 6 November 2001

2.1. IMF

[8] Figure 1 shows the magnitude of total and three components of the interplanetary magnetic field measured by ACE at 223Re on 6 November 2001. The solar wind shock arrived at 0124 UT, when the total magnetic field increased abruptly (top). The Bz component of the IMF became −61.4 nT, then reached a minimum of −77.0 nT at 0240 UT (bottom). IMF Bz remained southward until about 05 UT with the second minimum of −41.0 nT at 0420 UT. The solar wind shock caused an increase in the ground magnetic field at 0152 UT as seen in the SYM-H (Figure 2). The time lag between the shock detected by ACE and the ground magnetic effect was 28 min, which should be taken into account when we discuss the IMF driven convection electric field in the following sections. We here focus on the two time intervals, 0125–0300 UT and 0300–0500 UT, in

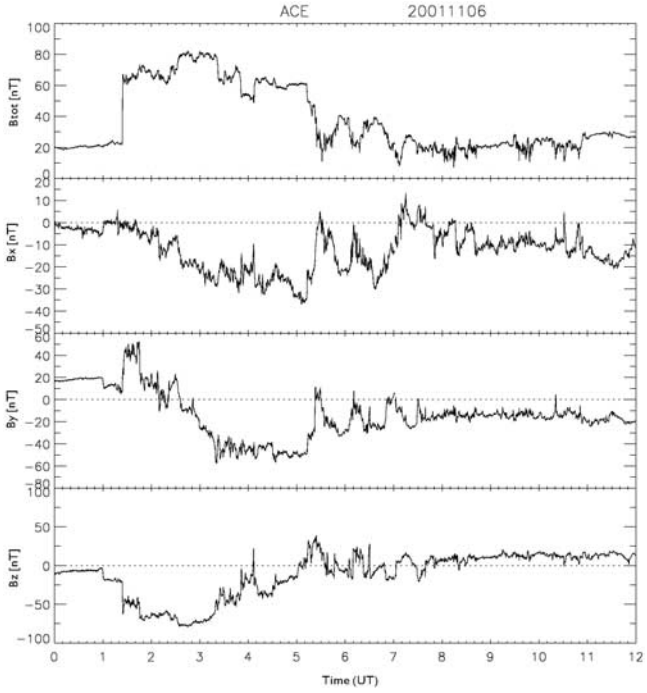

Figure 1. The interplanetary magnetic field (IMF) observed by ACE at x = 223 Re is shown for the time interval of 0–12 UT on 6 November 2001. From the top are shown the total B, and Bx, By and Bz components. The solar wind shock arrived at 0124 UT accompanying an abrupt increase in the southward IMF of −61.4 nT, which then reached a minimum of −77.0 nT at 0240 UT. The solar wind shock caused the SC on the ground 28 min after (see text).

which the magnetometer data are used to infer the state of the polar cap potential.

2.2. Ring Current

[9] The intense southward IMF caused a geomagnetic storm. Figure 2 shows a plot of the SYM-H provided by the WDC C2 for geomagnetism, Kyoto, which is derived from

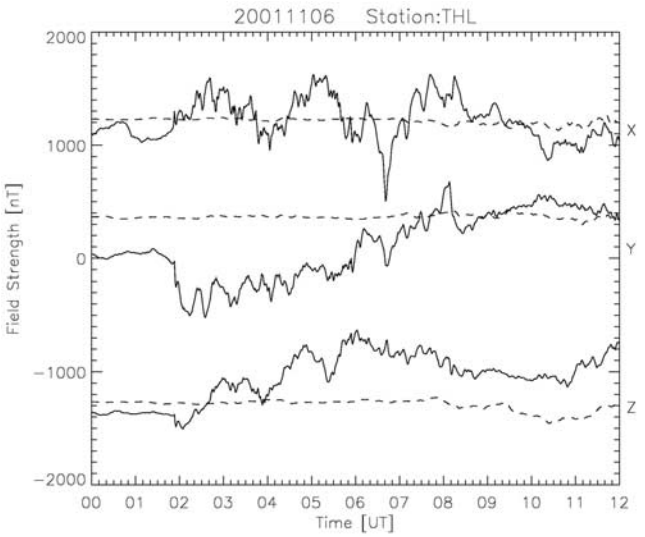

Figure 3. X, Y, and Z components of the magnetic field at the polar cap station, Thule (THL, 85.22° CGML, 2257 MLT at 02 UT) on the disturbed day (solid curves) and the quiet day (5 November 2001 shown with the dotted curves). The increases in the X over the time intervals of 0150–0340 and 0410–0550 indicate increases in the polar cap potential caused by the southward IMF.

magnetic X components recorded at middle and low latitudes. The SYM-H represents a symmetric component of the ring current. It is observed that the geomagnetic sudden commencement (SC) started at 0152 UT with the amplitude of 89 nT, followed by the steep decrease continuing for 80 min with the minimum of −330 nT at 0310 UT as measured from the peak of the SC. This steep decrease in the SYM-H was caused by the ring current that must have been developed by the electric field produced by the southward IMF in the first time interval.

2.3. Polar Cap Potential

[10] Figure 3 indicates X, Y, and Z components of the magnetic field at Thule (THL, 85.22° CGML, 2257 MLT at

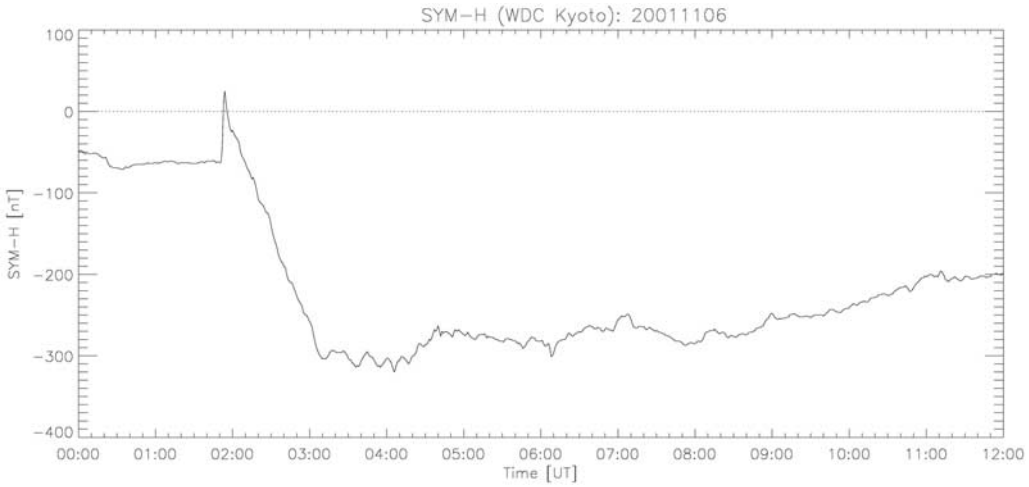

Figure 2. SYM-H for the time interval of 00–12 UT on 6 November 2001. The SC started at 0152 UT, 28 min after the shock arrived at ACE. The amplitude of the SC was 89 nT, and the SYM-H decreased steeply to a minimum of −330 nT at 0310 UT as measured from peak of the SC.

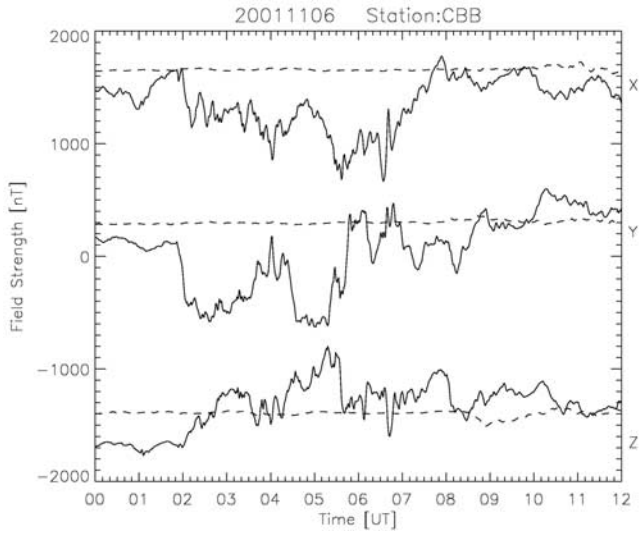

Figure 4. X, Y, and Z components of the magnetic field at the polar cap station, Cambridge Bay (CBB, 77.21° CGML, 1804 MLT at 02 UT) on the disturbed day (solid curves) and the quiet day (5 November 2001 shown with the dotted curves). The increases in the Y in the time intervals, 0150–0340 UT and 0410–0550 UT indicate increases in the polar cap potential caused by the southward IMF.

02 UT) on the disturbed day (solid curves) and quiet day (dashed curves). The X component started to increase at 0152 UT with an impulse corresponding to the SC, and increased over the two time intervals, 0150–0340 UT (hereafter denoted simply as 02–04 UT) and 0410–0550 UT (likewise 04–06 UT) with two broad maxima at 0240 and 0500 UT, which were caused by the increases in the southward IMF. The Y component, on the other hand, decreased over these time periods. Considering that THL was located at around the midnight (23–03 MLT) in the polar cap and that the declination of the geomagnetic field at THL was −57.02°, we infer that the magnetic disturbance vector was roughly directed toward the geomagnetic north. The R1 FACs expanded equatorward to 60° CGML (see 2.4), and therefore, THL (85.22° CGML) was located near the center of the pair of the R1 FACs. Thus the estimated magnetic disturbance vector could be caused by the Biot-Savart's effects of the R1 FACs.

[11] Figure 4 indicates X, Y, and Z components of the magnetic field at Cambridge Bay (CBB, 77.21° CGML, 1804 MLT at 02 UT) on the disturbed day (solid curves) and the quiet day (dashed curves). The Y component decreased over the two time intervals with minima at 0230 and 0500 UT, while the X component decreased over the first time interval and increased over the second time interval. The station was located in the local time sectors, 18–22 MLT in these time intervals and the declination of the geomagnetic field at CBB is 11.38°. Thus the decreases in the Y component are well explained by the Biot-Savart's effects of the R1 FACs that were located equatorward of the CBB. Likewise, the increase in the X component in the second time interval (premidnight) is explained by means of the R1 FACs.

[12] It should be noted that the X component at THL and the Y component at CBB are larger in amplitude for the second time interval, 04–06 UT, although the corresponding southward IMF was of smaller amplitude than that for the first time interval (Figure 1). This may imply that the R1 FACs were located closer to these stations in the second time interval.

2.4. Electrojets at Auroral and Midlatitudes

[13] Figure 5 shows the X component of the magnetic field from the IMAGE magnetometer chain (Table 1). The westward auroral electrojet started to increase at the same time as the SC, with intensification in the two time intervals, 02–04 and 04–06 UT, corresponding to the increases in the southward IMF (Figure 1). At the onset of the SC, 0152 UT (0430 MLT), the westward electrojet was intensified at midlatitude stations, HAN, NUR (57° CGML) with maximum amplitude of 2000 nT at 0300UT. On the other hand, the X-component at auroral latitude (e.g., OUJ, PEL) did not decrease significantly except for the quasiperiodic fluctuations. This latitudinal feature implies that the R1 FACs were located at about 60° CGML, and therefore, the westward electrojet was located at subauroral to midlatitudes, far equatorward from the typical auroral oval for this local time.

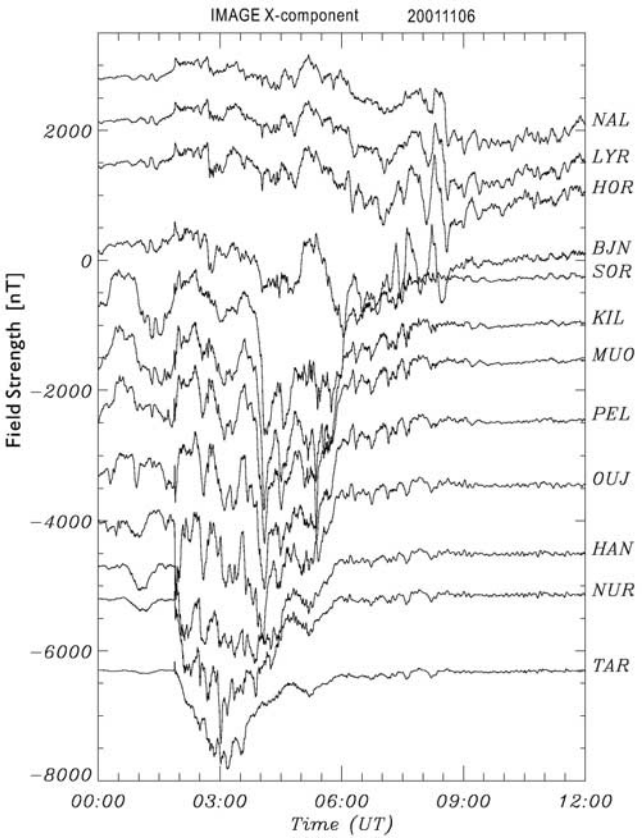

Figure 5. X-components of the 12 IMAGE magnetometers in the morning sector (MLT = UT + 2.5). Intense westward electrojets were observed at the subauroral and midlatitude stations, HAN (58.71° CGML), NUR (56.89°) and TAR (54.47°) for the first time interval (02–04UT), while the westward electrojet was observed at the auroral latitude stations, SOR (67.34°), KIL (65.88°) and MUO (64.72°), for the second time interval (04–06UT).

Table 1. List of the INTERMAGNET, IMAGE, and NICT SWM Magnetometer Stations

Station	Geographic Latitude	Geographic Longitude	Corr. Geomagnetic Latitude	Corr. Geomagnetic Longitude	MLT
Intermagnet					
CBB Cambridge Bay	69.10	255.00	77.21	309.16	UT−7.92
THL Thule	77.48	290.83	85.22	31.48	−3.05
IMAGE magnetometer chain					
NAL Ny Alesund	78.92	11.95	75.25	112.08	UT + 3.2
LYR Longyearbyen	78.20	15.82	75.12	113.00	+3.3
HOR Hornsund	77.00	15.60	74.13	109.59	+3.1
BJN Bear Island	74.50	19.20	71.45	108.07	+3.0
SOR Soroya	70.54	22.22	67.34	106.17	+2.5
KIL Kilpisjarvi	69.02	20.79	65.88	103.79	+2.2
MUO Muonio	68.02	23.53	64.72	105.22	+2.3
PEL Pello	66.90	24.08	63.55	104.92	+2.2
OUJ Oulujarvi	64.52	27.23	60.99	106.14	+2.3
HAN Hankasalmi	62.30	26.65	58.71	104.61	+2.2
NUR Nurmijarvi	60.50	24.65	56.89	102.18	+2.0
TAR Tartu	58.26	26.46	54.47	102.89	+2.1
NSWM magnetometers					
	Geographic		Geomagnetic		LT
OKI Okinawa	24.75	125.33	14.47	195.67	UT + 8.4
GAM Guam	13.58	144.87	4.89	215.26	+9.7
YAP Yap, Micronesia	9.3	138.5	−0.3	209.0	+9.2

[14] Two hours later, at 04 UT, the westward electrojet at the midlatitude decayed rapidly, and the westward electrojet was driven at auroral latitudes over SOR (67° CGML), MUO, and PEL with maximum amplitude of 2000 nT. This rapid movement of the westward electrojet occurred, when the polar cap potential decreased significantly as observed from the polar cap magnetometer data (Figures 3 and 4). It should be noted that the first electrojet intensification at the midlatitude occurred in the first time interval of the enhanced polar cap potential, 02–04 UT, i.e., during the main phase of the storm (Figure 2), which agrees with the typical equatorward movement of the electrojet during the major geomagnetic storms [*Feldstein et al.*, 1997]. On the other hand, the second electrojet intensification at the auroral latitude occurred during the period of the second enhancement of the polar cap potential (PCP) in the beginning of the recovery phase of the storm. It should be noted that the center of the AEJ moved rapidly poleward from 57° to 67° within 10 min.

2.5. Equatorial DP2 and CEJ

[15] To identify the DP2 currents at the low latitude and equator, we used the NICT Space Weather Monitoring (NSWM) magnetometers installed at the geomagnetic equator, Yap ((YAP, 0.3°S GML, Table 1) and Guam (GAM, 4.89°N GML), and at low latitude, Okinawa (OKI, 14.47°N GM). Figure 6 shows the H-component of the magnetic field recorded at OKI, GAM, and YAP. The SC started at 0152 UT (1052 LT) with an amplitude of 70 nT at OKI, then the H-component decreased steeply for 2 h and reached a minimum of −280 nT at around 0410 UT (1310 LT), as measured from the peak of the SC. The amplitude of the geomagnetic storm is smaller and the time of the minimum is delayed as compared with those of the SYM-H (Figure 2), which may be due to local time asymmetry of the ring current. The ring current responsible for the steep decrease in the magnetic field developed immediately after the SC, concurrently with the increase in the PCP. The ring current then ceased developing when the southward IMF decreased at the end of the first time interval. The quick development of the ring current shown in Figures 2 and 6 may indicate prompt penetration of the convection electric field into the inner magnetosphere.

[16] In contrast to the steep decrease in the H-component at OKI, the H-component at the geomagnetic equator, YAP located at the same local time as OKI, remained high with amplitude of 230 nT for an hour and then decreased more steeply than that at OKI (Figure 6). As a result, the size of the geomagnetic storm was 760 nT at YAP as measured from the peak of the SC to the minimum of the magnetic deflection, which is 2.7 times the size of the geomagnetic storm at OKI. It should be noted that the H-component at YAP remained at high level while the ring current was well developing (Figures 2 and 6). The excess part of the magnetic field at YAP may be a signature of the ionospheric DP2 currents superposed on the ring current effects that appear dominantly at OKI.

[17] To derive the DP2 currents at the dayside geomagnetic equator, we subtract the quiet time diurnal variation (Sq) and magnetic perturbations due to magnetospheric currents from the geomagnetic storm at YAP. We assume that the geomagnetic storm recorded at OKI is composed only of magnetospheric ring currents, since the DP2 at low latitude is of much smaller magnitude than at the geomag-

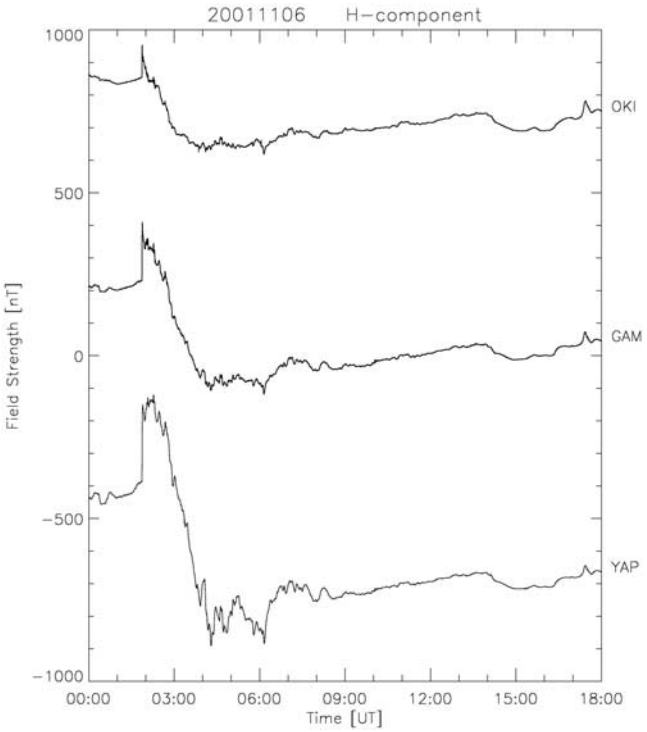

Figure 6. H-component of the magnetic field at the low latitude, OKI (14.47° GML), and near the geomagnetic equator, GA M (4.89°), YAP (−0.3°), which were located at around noon, when the storm started (MLT = UT + 9). The storm-time ring current developed immediately after the SC at OKI, while the equatorial electrojet was intensified during the main phase. The size of the geomagnetic storm was remarkably amplified at the geomagnetic equator (see text).

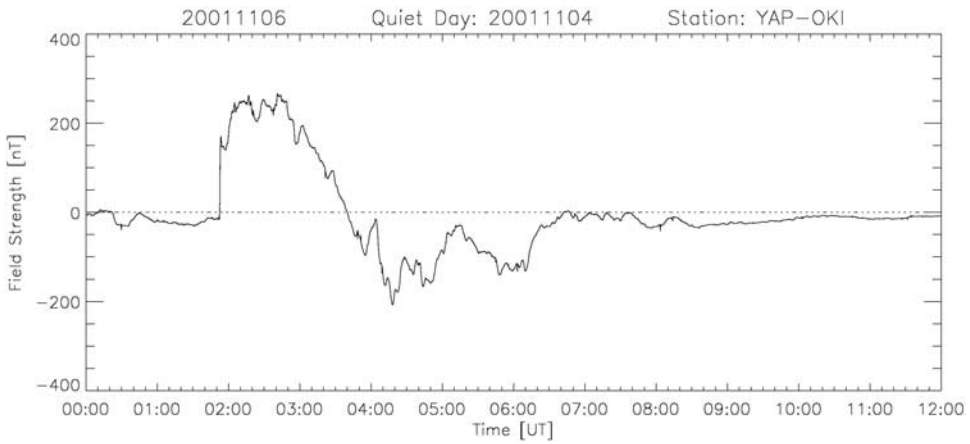

Figure 7. Magnetic deflections caused by the ionospheric currents at the equator, YAP (−0.3° GML). Quiet time magnetic variations on 4 November 2001 were subtracted from the geomagnetic storm, and effects of the magnetospheric current were eliminated by subtracting the low latitude geomagnetic disturbances recorded at OKI (14.47°). The resultant magnetic disturbances were composed of eastward currents during the storm main phase and westward currents during the recovery phase.

netic equator [see *Kikuchi et al.*, 1996]. We further assume that the magnetospheric currents produce the same amplitude of the geomagnetic perturbations at OKI and YAP, because of short latitudinal distance between these two stations (14.8°). Then we obtain the equatorial DP2 during the geomagnetic storm as shown in Figure 7. It is observed that the DP2 was considerably enhanced during the main phase when YAP was located at 11–13 LT, with a peak amplitude of 280 nT, but it started to decrease one hour after the SC and turned to negative, i.e., CEJ, at 0340 UT (1240 LT) with a peak amplitude of about 190 nT at 0415UT (1315 LT). This result implies predominance of a dawn-to-dusk electric field during the main phase and a dusk-to-dawn electric field during the recovery phase, which drove eastward and westward electrojets in the dayside equatorial ionosphere. There have been several papers dealing with model calculations for the direct penetration and overshielding electric field and currents at the equator by giving the R1 and R2 FACs [*Nopper and Carovillano*, 1978; *Tsunomura*, 1999; *Senior and Blanc*, 1984; *Peymirat et al.*, 2000]. According to the calculation by *Peymirat et al.* [2000], the convection electric field at the equator is eastward in a time interval 8–22 LT, which drives eastward currents over 8–18 LT depending on the ionospheric conductivity. On the other hand, the electric field became negative over 4–19 LT, immediately after the decrease in the PCP. The electric current is reversed in direction in a time interval 6–18 LT. YAP and OKI were located at 11–13 LT during the DP2 and at 13–16 LT during the CEJ. The decrease in the DP2 during the latter half of the main phase implies growth of the shielding electric field before the occurrence of the CEJ. It is remarkable that the DP2 was greater than the size of the quiet time diurnal magnetic field variation (220 nT) at YAP, indicating that the stormtime electric field overwhelmed the dynamo electric field at the equator.

[18] The equatorial CEJ occurred, when the R1 FACs decreased substantially as inferred from the decrease in the PCP (Figures 3 and 4), and continued for 3 h in the beginning of the recovery phase. It should be noted that the southward IMF decreased its magnitude, but remained southward with the magnitude of 40 nT at the onset of the equatorial CEJ. The occurrence of the CEJ under the condition of the southward IMF is a result of the substantial development of the shielding electric field during the late main phase. If the PCP remained constant, the overshielding would not be significant, but could appear because the shielding/overshielding depends on the location relative to the R1 and R2 FACs. It should be noted that the increase in the PCP in the second time interval, 04–06 UT (Figures 3 and 4) caused only a minor development of the ring current during the period of the CEJ. From the dominant overshielding electric field at the equator we infer that the convection electric field in the inner magnetosphere was not strong to drive the ring current

2.6. Relationship Between the AEJ and the Equatorial DP2/CEJ

[19] In order to see the relationship between the strength of the AEJ and the equatorial DP2/CEJ in more detail, we plot contours of the AEJ in the latitude-time coordinates, together with the equatorial DP2 (Figure 8). The AEJ was located at subauroral and midlatitude (55°–60° CGML) during the period of the equatorial DP2, while the AEJ shifted poleward to the auroral latitudes (60°–70°) during the period of the CEJ. The strength of the AEJ did not change considerably for the two time intervals, but the equatorial DP2 decreased to be overwhelmed by the shielding electric field for the second time interval. The poleward shift of the AEJ was very rapid in such a way that the center of the AEJ shifted from 57° to 67° in 10 min, which in turn implies a contraction of the auroral oval. As a result, the size of the polar electric field reduced and the smaller size results in more geometrical attenuation of the electric field penetrated to low latitude [*Kikuchi et al.*, 1978; *Kikuchi and Araki*, 1979]. Therefore the overshielding effect must be strengthened by the poleward shift of the R1 FACs.

3. Discussion

[20] The equatorial DP2 current is a part of the global current system driven by the convection electric field in the

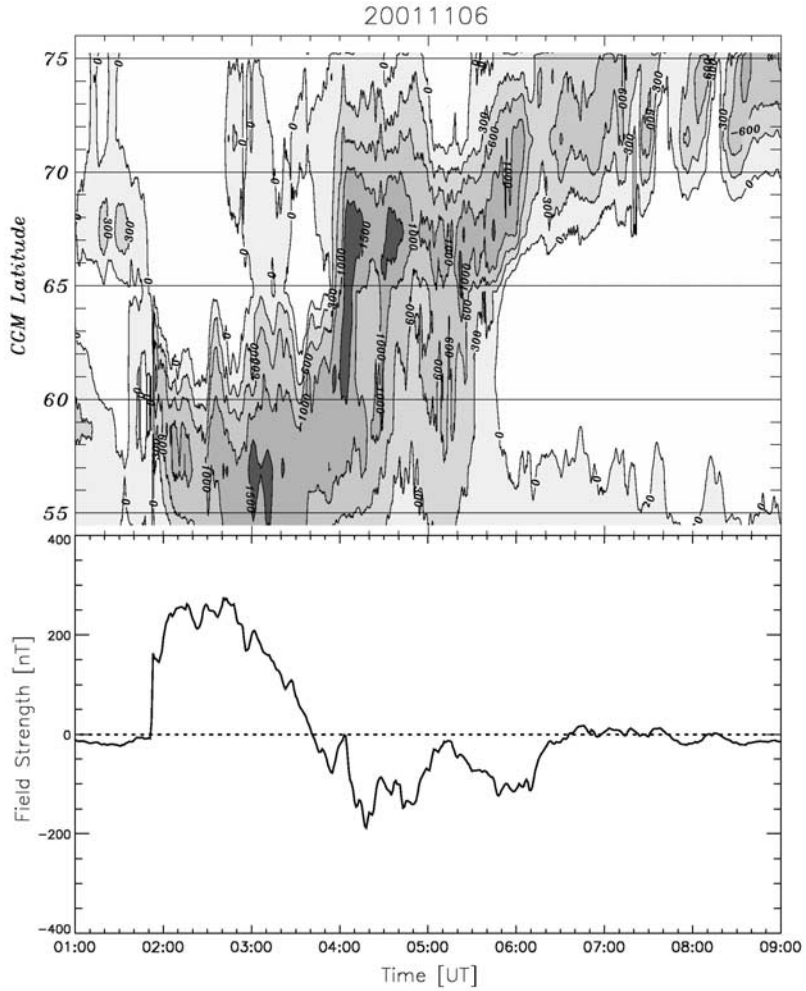

Figure 8. Contour map of the magnetic disturbances due to the westward electrojet at auroral-midlatitudes in the dawn sector (top), and magnetic disturbances due to the equatorial DP2/CEJ currents (bottom). The westward electrojet developed at midlatitudes concurrently with the equatorial DP2, while it shifted to the auroral latitude during the period of the equatorial CEJ. The DP2 started to decrease one hour after the storm onset when the auroral electrojet was still growing.

polar ionosphere [*Nishida et al.*, 1966; *Kikuchi et al.*, 1996]. *Kikuchi et al.* [1996] showed that the DP2 current circuit was completed near-instantaneously within the temporal resolution of 25 s. Extremely strong DP2 currents were driven simultaneously in the polar cap (Figures 3 and 4) and at auroral to equatorial latitudes (Figures 5 and 7) during the geomagnetic storm on 6 November 2001. In particular, the westward electrojet started to develop at subauroral to midlatitude (<60° CGML) in the dawn sector, right after the arrival of the southward IMF. This may indicate that the R1 FACs developed at 60° CGML (L = 4), although the R1 FACs developed at around 72° (L = 10.5) for a substorm event [e.g., *Kikuchi et al.*, 1996]. This inevitably leads to the R2 FACs and ring current development to occur deep in the inner magnetosphere (L = 3 or less). Indeed, the CRRES and Akebono satellites have detected intense electric fields at L = 2–3 responsible for the development of the ring current [*Burke et al.*, 1998; *Wilson et al.*, 2001; *Shinbori et al.*, 2005]. *Shinbori et al.* [2005] showed that the Akebono detected an electric field of the magnitude of up to 28 mV/m at around L = 2.5 during the main phase of the major geomagnetic storm on 13 March 1989.

[21] The concurrent development of the DP2 currents and the ring current was studied for a substorm by *Hashimoto et al.* [2002]. *Hashimoto et al.* [2002] demonstrated that the asymmetric ring current started to develop within a few minutes after the PCP and midlatitude DP2 started to grow because of the southward turning of the IMF. They further indicated that the asymmetric ring current was caused by an asymmetric distribution of the high pressure plasma in the inner magnetosphere using the *Ebihara and Ejiri* [2000] ring current model. When the IMF turned northward, the PCP decreased and the asymmetric ring current immediately started to change into symmetric in local time. *Hashimoto et al.* [2002] suggested that the convection electric field was transmitted to the inner magnetosphere via the midlatitude ionosphere. The simultaneous increase in the PCP and the equatorial DP2 shown above is in good agreement with the results of *Hashimoto et al.* [2002].

[22] The transmission of the ionospheric electric field into the inner magnetosphere was discussed by *Kikuchi* [2005]

using the Earth-ionosphere waveguide model for the instantaneous transmission of the polar electric field to the equator [*Kikuchi et al.*, 1978; *Kikuchi and Araki*, 1979]. The TM_0 mode waves propagate at the speed of light, accompanying electric currents in the ionosphere and on the surface of the ground. An electric field is deduced from the ionospheric current and will be transmitted to the inner magnetosphere along the magnetic field lines. Thus the quick development of the ring current shown above is explained by means of the electric field transmitted from the ionosphere.

[23] The development of the ring current drives FACs that flow into the ionosphere and produce an electric field directed opposite to the convection electric field [*Vasyliunas*, 1972]. This electric field is transmitted to low latitude instantaneously, and tends to cancel the convection electric field. The shielding electric field occasionally causes the overshielding when the convection electric field decreased rapidly [*Kelley et al.*, 1979; *Gonzales et al.*, 1979; *Fejer et al.*, 1979; *Kobea et al.*, 2000; *Kikuchi et al.*, 2000b, 2003]. The shielding electric field starts to grow a few minutes after the enhancement of the convection electric field, but it would need some time to make significant effects at low latitude, particularly during a period of growing convection electric field. The analyses of the substorm have indicated that the shielding time constant was about 17–20 min for the growth phase of the substorm [*Somayajulu et al.*, 1987; *Kikuchi et al.*, 2000b]. Model calculations indicated that the shielding time constant was proportional to the ionospheric conductance and inversely proportional to the density and temperature of the plasma sheet [*Jaggi and Wolf*, 1973; *Southwood*, 1977; *Senior and Blanc*, 1984; *Peymirat et al.*, 2000]. The time constant thus obtained was about 20 min [*Senior and Blanc*, 1984]. However, *Huang et al.* [2005] indicated that the time constant was 2–4 h for geomagnetic storms, much longer than those reported previously for substorms. The extremely strong westward electrojet (Figure 5) imply that the auroral ionosphere was highly ionized, which could result in longer time constant and enabled the convection electric field to penetrate to the equator during the main phase. However, the shielding electric field became effective 1 h after the onset of the main phase, although the southward IMF remained strong (−70 nT) and the SYM-H was still decreasing. The well-developed shielding electric field then caused the CEJ in the beginning of recovery phase, when the PCP decreased because of the decrease in the southward IMF.

[24] The overshielding is usually caused by the northward turning of the IMF, which would reduce the magnitude of the PCP [*Kelley et al.*, 1979]. It should be noted that the overshielding analyzed above occurred when the IMF remained southward with large magnitude (40 nT), and the deflection in the polar cap magnetic field was even larger during the period of the CEJ. The abrupt poleward shift of the auroral oval by 10° reduced the size of the polar cap, which would reduce the electric field at low latitude because of the geometrical attenuation of the penetrated electric field [*Kikuchi et al.*, 1978]. Consequently, the development of the storm-time ring current that depends on the electric field penetrated to mid and low latitude becomes weaker irrespective of the electric field in the polar cap.

[25] On the other hand, the equatorial CEJ could also be caused by the disturbance dynamo as pointed out by *Huang et al.* [2005]. Since the disturbance dynamo is driven by the thermospheric wind from the auroral ionosphere [*Blanc and Richmond*, 1980], it takes several hours for the dynamo to become effective and the dynamo continues to work for longer time, say, for ten hours during the geomagnetic storm [*Fejer and Scherliess*, 1997]. It should be noted that the CEJ reported above continued for three hours (04–07 UT), which may not agree with the disturbance dynamo, but agrees with the overshielding due to the R2 FACs [e.g., *Peymirat et al.*, 2000].

[26] *Rastogi* [2004] demonstrated that the magnitude of the geomagnetic storm was significantly enhanced at the dayside geomagnetic equator, which was attributed to the CEJ caused by the northward turning of the IMF. The CEJ that occurred at the end of the main phase of the storm analyzed above agrees with the scenario of *Rastogi* [2004]. However, detailed analysis of the equatorial geomagnetic storm revealed that the strong eastward DP2 currents were associated with the main phase (Figure 7), which amplified the geomagnetic storm considerably at the dayside geomagnetic equator. On the other hand, the diurnal variation at the geomagnetic equator is substantially depressed during disturbed periods [*Matsushita and Balsley*, 1972; *Onwumechilli et al.*, 1973; *Kikuchi et al.*, 1996]. The depression of the daily variation may be caused by the disturbance dynamo electric field. If the disturbance dynamo worked during the main phase, it could act against the effect of the DP2 currents, and as a result, the equatorial enhancement of the geomagnetic storm must be caused only by the CEJ as pointed out by *Rastogi* [2004]. The outstanding equatorial enhancement shown in the present paper suggests no significant contribution of the disturbance dynamo electric field on the geomagnetic storm.

4. Conclusion

[27] By subtracting the geomagnetic storm at low latitude, Okinawa, from that at the dayside geomagnetic equator, Yap, we deduced several outstanding features of the geomagnetic storm as shown below.

[28] 1. During the main phase of the geomagnetic storm, the convection electric field drove the electrojet of the magnitude of 2000 nT at midlatitude centered at 57° CGML in the dawn sector. This implies equatorward expansion of the R1 FACs, which caused penetration of intense convection electric field to the equator, and drove the DP2 currents at the dayside geomagnetic equator with magnitude greater than the diurnal variation. It is remarkable that the ring current started to develop within a few minutes after the increase in the DP2 currents, which suggests that the ionospheric electric field responsible for the DP2 currents played a crucial role in the development of the ring current.

[29] 2. The shielding became effective one hour after the onset of the equatorial DP2, in contrast to several hours of the shielding time constant suggested by *Huang et al.* [2005]. The well developed shielding electric field during the main phase resulted in the overshielding when the southward IMF decreased its magnitude in the beginning of the recovery phase.

[30] 3. The overshielding occurred when the magnitude of the southward IMF decreased, but remained strong (40 nT). It should be stressed that the location of the R1

FACs shifted from 60° to 70° in 10 min. The rapid poleward shift of the R1 FACs results in a decrease in size of the polar electric field and causes considerable geometrical attenuation of the penetrated electric field at low latitude.

[31] 4. The geomagnetic storm was substantially amplified as compared with the low latitude storm by a factor of 2.7. The amplification of the geomagnetic storm is usually caused by the CEJ in the beginning of the recovery phase, but the geomagnetic storm on 6 November 2001 was further amplified by the DP2 current during the main phase.

[32] **Acknowledgments.** We would like to thank the Finnish Meteorological Institute for the IMAGE magnetometer data, and thank the U.S. NOAA/Weather Service Office at Yap and P. Hattori at the USGS/Guam Magnetic Observatory for their help in operating the magnetometers for space weather monitoring of the National Institute of Information and Communications Technology. The SYM-H was provided by the WDC for Geomagnetism, Kyoto. INTERMAGNET data used in this paper are obtained from the 2001 CD-ROM. The ACE level 2 data were obtained through the Coordinated Data Analysis Web (CDAWeb).

[33] Wolfgang Baumjohann thanks Mangalathayil Ali Abdu, Michael Blanc and Rudolf Treumann for their assistance in evaluating this paper.

References

Araki, T. (1977), Global structure of geomagnetic sudden commencements, *Planet. Space Sci.*, *25*, 373–384.

Araki, T. (1994), A physical model of the geomagnetic sudden commencement, solar wind sources of magnetospheric ultra-low-frequency waves, *Geophys. Monogr.*, *81*, 183–200.

Baker, W. G., and D. F. Martyn (1953), Electric currents in the ionosphere. Part I: The conductivity, *Philos. Trans. R. Soc. Ser. A and Ser. B*, *246*, 281–294.

Blanc, M., and A. D. Richmond (1980), The ionospheric disturbance dynamo, *J. Geophys. Res.*, *85*(A4), 1669–1686.

Burke, W. J., N. C. Maynard, M. P. Hagan, R. A. Wolf, G. R. Wilson, L. C. Gentile, M. S. Gussenhoven, C. Y. Huang, T. W. Garner, and F. J. Rich (1998), Electrodynamics of the inner magnetosphere observed in the dusk sector by CRRES and DMSP during the magnetic storm of June 4–6, 1991, *J. Geophys. Res.*, *103*(A12), 29,339–29,418.

Ebihara, Y., and M. Ejiri (2000), Simulation study on fundamental properties of the storm-time ring current, *J. Geophys. Res.*, *105*(A7), 15,843–15,859.

Fejer, B. G., and L. Scherliess (1997), Empirical models of storm time equatorial zonal electric fields, *J. Geophys. Res.*, *102*(A11), 24,047–24,056.

Fejer, B. G., C. A. Gonzales, D. T. Farley, M. C. Kelley, and R. Woodman (1979), Equatorial electric fields during magnetically disturbed conditions: 1. The effect of the interplanetary magnetic field, *J. Geophys. Res.*, *84*(A10), 5797–5802.

Feldstein, Y. I., A. Grafe, L. I. Gromova, and V. A. Popov (1997), Auroral electrojets during geomagnetic storms, *J. Geophys. Res.*, *102*(A7), 14,223–14,235.

Gonzales, C. A., M. C. Kelley, B. G. Fejer, J. F. Vickrey, and R. F. Woodman (1979), Equatorial electric fields during magnetically disturbed conditions: 2. Implications of simultaneous auroral and equatorial measurements, *J. Geophys. Res.*, *84*(A10), 5803–5812.

Hashimoto, K. K., T. Kikuchi, and Y. Ebihara (2002), Response of the magnetospheric convection to sudden interplanetary magnetic field changes as deduced from the evolution of partial ring currents, *J. Geophys. Res.*, *107*(A11), 1337, doi:10.1029/2001JA009228.

Hirono, M. (1952), A theory of diurnal magnetic variations in equatorial regions and conductivity of the ionosphere E region, *J. Geomagn. Geoelectr.*, *4*, 7–21.

Huang, C.-S., J. C. Foster, and J. M. Holt (2001), Westward plasma drift in the midlatitude ionospheric F region in the midnight-dawn sector, *J. Geophys. Res.*, *106*(A12), 30,349–30,362.

Huang, C.-S., J. C. Foster, and M. C. Kelley (2005), Long-duration penetration of the interplanetary electric field to the low-latitude ionosphere during the main phase of magnetic storms, *J. Geophys. Res.*, *110*, A11309, doi:10.1029/2005JA011202.

Jaggi, R. K., and R. A. Wolf (1973), Self-consistent calculation of the motion of a sheet of ions in the magnetosphere, *J. Geophys. Res.*, *78*(16), 2852–2866.

Kelley, M. C., B. G. Fejer, and C. A. Gonzales (1979), An explanation for anomalous equatorial ionospheric electric fields associated with a northward turning of the interplanetary magnetic field, *Geophys. Res. Lett.*, *6*(4), 301–304.

Kikuchi, T. (2005), Transmission line model for driving plasma convection in the inner magnetosphere, in *The Inner Magnetosphere: Physics and Modeling*, *Geophys. Monogr. Ser.*, vol. 155, edited by T. I. Pulkkinen, N. A. Tsyganenko, and R. H. W. Friedel, pp. 173–179, AGU, Washington, D. C.

Kikuchi, T., and T. Araki (1979), Horizontal transmission of the polar electric field to the equator, *J. Atmos. Sol. Terr. Phys.*, *41*, 927–936.

Kikuchi, T., T. Araki, H. Maeda, and K. Maekawa (1978), Transmission of polar electric fields to the equator, *Nature*, *273*, 650–651.

Kikuchi, T., H. Lühr, T. Kitamura, O. Saka, and K. Schlegel (1996), Direct penetration of the polar electric field to the equator during a DP2 event as detected by the auroral and equatorial magnetometer chains and the EISCAT radar, *J. Geophys. Res.*, *101*(A8), 17,161–17,173.

Kikuchi, T., M. Pinnock, A. Rodger, H. Luehr, T. Kitamura, H. Tachihara, M. Watanabe, N. Sato, and M. Ruohoniemi (2000a), Global evolution of a substorm-associated DP2 current system observed by SuperDARN and magnetometers, *Adv. Space Res.*, *26*, 121–124.

Kikuchi, T., H. Luehr, K. Schlegel, H. Tachihara, M. Shinohara, and T.-I. Kitamura (2000b), Penetration of auroral electric fields to the equator during a substorm, *J. Geophys. Res.*, *105*(A10), 23,251–23,261.

Kikuchi, T., K. K. Hashimoto, T.-I. Kitamura, H. Tachihara, and B. Fejer (2003), Equatorial counterelectrojets during substorms, *J. Geophys. Res.*, *108*(A11), 1406, doi:10.1029/2003JA009915.

Kobea, A. T., C. Amory-Mazaudier, J. M. Do, H. Luehr, E. Hougninou, J. Vassal, E. Blanc, and J. J. Curto (1998), Equatorial electrojet as part of the global circuit: A case-study from the IEEY, *Ann. Geophys.*, *16*, 698–710.

Kobea, A. T., A. D. Richmond, B. A. Emery, C. Peymirat, H. Luehr, T. Moretto, M. Hairston, and C. Amory-Mazaudier (2000), Electrodynamic coupling of high and low latitudes: Observations on May 27, 1993, *J. Geophys. Res.*, *105*(A10), 22,979–22,989.

Matsushita, S., and B. B. Balsley (1972), A question of DP2 magnetic fluctuations, *Planet. Space Sci.*, *20*, 1259–1267.

Motoba, T., T. Kikuchi, H. Lühr, H. Tachihara, T.-I. Kitamura, K. Hayashi, and T. Okuzawa (2002), Global Pc5 caused by a DP2-type ionospheric current system, *J. Geophys. Res.*, *107*(A2), 1032, doi:10.1029/2001JA900156.

Motoba, T., T. Kikuchi, T. S. Fukuda, and K. Yumoto (2004), HF Doppler oscillations in the low-latitude ionosphere coherent with equatorial long-period geomagnetic field oscillations, *J. Geophys. Res.*, *109*, A06214 doi:10.1029/2004JA010442.

Nishida, A. (1968), Coherence of geomagnetic DP2 magnetic fluctuations with interplanetary magnetic variations, *J. Geophys. Res.*, *73*(17), 5549–5559.

Nishida, A., N. Iwasaki, and T. Nagata (1966), The origin of fluctuations in the equatorial electrojet: A new type of geomagnetic variation, *Ann. Geophys.*, *22*, 478–484.

Nopper, R. W., and R. L. Carovillano (1978), Polar-equatorial coupling during magnetically active periods, *Geophys. Res. Lett.*, *5*(8), 699–702.

Onwumechilli, A., K. Kawasaki, and S.-I. Akasofu (1973), Relationships between the equatorial electrojet and polar magnetic variations, *Planet. Space Sci.*, *21*, 1–16.

Peymirat, C., A. D. Richmond, and A. T. Kobea (2000), Electrodynamic coupling of high and low latitudes: Simulations of shielding/overshielding effects, *J. Geophys. Res.*, *105*(A10), 22,991–23,003.

Rastogi, R. G. (1977), Geomagnetic storms and electric fields in the equatorial ionosphere, *Nature*, *268*, 422–424.

Rastogi, R. G. (1997), Midday reversal of equatorial ionospheric electric field, *Ann. Geophys.*, *15*, 1309–1315.

Rastogi, R. G. (2004), Westward electric field in the low latitude ionosphere during the main phase of magnetic storms occurring around local midday hours, *Sci. Lett.*, *27*, 69–74.

Rastogi, R. G., and V. L. Patel (1975), Effect of interplanetary magnetic field on ionosphere over the magnetic equator, *Proc. Indian Acad. Sci.*, *82*, 121–141.

Senior, C., and M. Blanc (1984), On the control of magnetospheric convection by the spatial distribution of ionospheric conductivities, *J. Geophys. Res.*, *89*(A1), 261–284.

Shinbori, A., Y. Nishimura, T. Ono, M. Iizima, A. Kumamoto, and H. Oya (2005), Electrodynamics in the duskside inner magnetosphere and plasmasphere during a super magnetic storm on March 13–15, 1989, *Earth Planets Space*, *57*, 643–659.

Somayajulu, V. V., C. A. Reddy, and K. S. Viswanathan (1987), Penetration of magnetospheric convective electric field to the equatorial ionosphere during the substorm of March 22, 1979, *Geophys. Res. Lett.*, *14*(8), 876–879.

Southwood, D. J. (1977), The role of hot plasma in magnetospheric convection, *J. Geophys. Res.*, *82*(35), 5512–5520.

Trivedi, N. B., B. R. Arora, A. L. Padilha, J. M. Da Costa, S. L. G. Dutra, F. H. Chamalaun, and A. Rigoti (1997), Global Pc5 geomagnetic pulsations of March 24, 1991, as observed along the American sector, *Geophys. Res. Lett.*, *24*(13), 1683–1686.

Tsunomura, S. (1999), Numerical analysis of global ionospheric current system including the effect of equatorial enhancement, *Ann. Geophys.*, *17*, 692–706.

Tsurutani, B., et al. (2004), Global dayside ionospheric uplift and enhancement associated with interplanetary electric fields, *J. Geophys. Res.*, *109*, A08302, doi:10.1029/2003JA010342.

Vasyliunas, V. M. (1972), The interrelationship of magnetospheric processes, in *Earth's Magnetospheric Processes*, edited by B. M. McCormac, pp. 29–38, D. Reidel, Norwell, Massachusetts.

Wilson, G. R., W. J. Burke, N. C. Maynard, C. Y. Huang, and H. J. Singer (2001), Global electrodynamics observed during the initial and main phases of the July 1991 magnetic storm, *J. Geophys. Res.*, *106*(A11), 24,517–24,539.

Wygant, J., D. Rowland, H. J. Singer, M. Temerin, F. Mozer, and M. K. Hudson (1998), Experimental evidence on the role of the large spatial scale electric field in creating the ring current, *J. Geophys. Res.*, *103*(A12), 29,527–29,544.

K. K. Hashimoto, School of Environment Management, Kibi International University, Takahashi, Okayama 716-8508, Japan. (hashi@kiui.ac.jp)

T. Kikuchi, Solar-Terrestrial Environment Laboratory, Nagoya University, Furo-cho, Chikusa-ku, Nagoya, Aichi 464-8601, Japan. (kikuchi@stelab.nagoya-u.ac.jp)

K. Nozaki, Applied Electromagnetic Research Center, National Institute of Information and Communications Technology, Koganei, Tokyo 184-8795, Japan. (nozaki@nict.go.jp)